Published in final edited form as:
Neuroscience. 2011 September 8; 190: 184–193. doi:10.1016/j.neuroscience.2011.06.018.

A restricted parabrachial pontine region is active during non-REM sleep

Pablo Torterolo[1], **Sharon Sampogna**[3], and **Michael H. Chase**[2,3]

[1]Departamento de Fisiología, Facultad de Medicina, Universidad de la República, General Flores 2125, 11800 Montevideo-Uruguay

[2]UCLA School of Medicine, Los Angeles, CA 90095

[3]WebSciences International, 1251 Westwood Blvd., Los Angeles, CA 90024

Abstract

The principal site that generates both REM sleep and wakefulness is located in the mesopontine reticular formation, whereas non-REM sleep (NREM) is primarily dependent upon the functioning of neurons that are located in the preoptic region of the hypothalamus. In the present study, we were interested in determining whether the occurrence of NREM might also depend on the activity of mesopontine structures, as has been shown for wakefulness and REM sleep.

Adult cats were maintained in one of the following states: quiet wakefulness (QW), alert wakefulness (AW), NREM, or REM sleep induced by microinjections of carbachol into the nucleus pontis oralis (REM-carbachol). Subsequently, they were euthanized and single labeling immunohistochemical studies were undertaken to determine state-dependent patterns of neuronal activity in the brainstem based upon the expression of the protein Fos. In addition, double labeling immunohistochemical studies were carried out to detect neurons that expressed Fos as well as choline acetyltransferase, tyrosine hydroxylase or GABA.

During NREM, only a few Fos immunoreactive cells were present in different regions of the brainstem; however, a discrete cluster of Fos+ neurons was observed in the caudolateral peribrachial region (CLPB). The number of the Fos+ neurons in the CLPB during NREM was significantly greater (67.9 ± 10.9, $P < 0.0001$) compared to QW (8.0 ± 6.7), AW (5.2 ± 4.2) or REM-carbachol (8.0 ± 4.7). In addition, there was a positive correlation ($R = 0.93$) between the time the animals spent in NREM and the number of Fos+ neurons in the CLPB. Fos-immunoreactive neurons in the CLPB were neither cholinergic nor catecholaminergic; however about 50% of these neurons were GABAergic.

We conclude that a group of GABAergic and unidentified neurons in the CLPB are active during NREM and likely involved in the control of this behavioral state. These data open new avenues for the study of NREM, as well as for the explorations of interactions between these neurons that are activated during NREM, and cells of the adjacent pontine tegmentum that are involved in the generation of REM sleep.

Please address correspondence to: Dr. Pablo Torterolo, Facultad de Medicina, Universidad de la República, General Flores 2125, 11800 Montevideo-Uruguay. TEL: (5982) 924 34 14 ext. 3234. ptortero@fmed.edu.uy.

Keywords

parabrachial; PGO; REM; slow wave sleep; GABA

In the early part of the 20th century, Von Economo studied the brains of individuals who were either unable to awaken from a sleep-like coma or had profound insomnia as a result of an influenza epidemic (Spanish flu). Based on his anatomical studies, which revealed abnormalities in the hypothalamus, Von Economo proposed that sleep is regulated by opposing sleep-promoting and wake-promoting mechanisms (Von Economo, 1930). Since then, several reports have shown that the preoptic region of the hypothalamus is a major center that controls the generation of non-REM sleep (NREM) (Szymusiak and McGinty, 2008). Experimental lesions of this area result in insomnia, whereas electrical, neurochemical or thermal stimulation elicit or increase NREM (ibid). Furthermore, electrophysiological studies as well as experiments dealing with the immediate early gene protein Fos have shown that neurons in this region are activated during NREM (Sherin et al., 1996; Szymusiak et al., 1998; Gong et al., 2000; Dentico et al., 2009; Torterolo et al., 2009a).

The mesopontine tegmentum is considered the main component of the ascending reticular activating system, which is critical for the generation of wakefulness (recently reviewed by Torterolo and Vanini, 2010). Within this area, there is also the “necessary and sufficient” circuitry, centered in the nucleus pontis oralis, that controls REM sleep generation (Siegel, 2005).

In the present study, utilizing Fos immunoreactivity as a marker of neuronal activity (Dragunow and Faull, 1989), we examined areas of the brainstem to determine whether there is selective neuronal activation during NREM. We found that a circumscribed site located in the caudolateral peribrachial region (CLPB), which has not previously been implicated in the control of NREM, exhibited striking NREM-dependent patterns of activity.

2. Experimental procedure

2.1. Experimental animals

Twenty adult male cats were determined to be in good health by veterinarians; all experimental procedures were conducted in accordance with the “Guide to the care and use of laboratory animals” (8th edition, National Academy Press, Washington D. C., 2010). Adequate measures were taken to minimize pain, discomfort or stress of the animals. In addition, we used the minimal number of animals necessary to produce reliable scientific data.

2.2. Surgical Procedures

The following surgical procedures were carried out in order to monitor states of sleep and wakefulness in chronic, anaesthetized cats. Prior to anesthetization, each cat was pre-medicated with xylazine® (2.2 mg/kg, i.m.), atropine (0.04 mg/kg, i.m.) and antibiotics (tribrissen®, 30 mg/kg, i.m.). Anesthesia, which was initially induced with ketamine (15 mg/kg, i.m.), was maintained with a gas mixture of isoflourane in oxygen (1-3%). The head was positioned in a stereotaxic frame and the skull was exposed. Stainless steel screw electrodes were placed in the frontal and parietal bones to record the electroencephalogram (EEG) and in the orbital portion of the frontal bone to record eye movements (electro-oculogram, EOG). Bipolar electrodes were implanted in both lateral geniculate nuclei in order to monitor ponto-geniculo-occipital (PGO) waves. A Winchester plug (connected to the electrodes) and a chronic head-restraining device were bonded to the skull with acrylic

cement. In selected animals, a small hole (5 mm in diameter) was placed in the skull overlying the cerebellar cortex; this hole was subsequently used to provide access to the pons for drug administration (Torterolo et al., 2000; Torterolo et al., 2009a). At the end of these surgical procedures, an analgesic (Buprenex®, 0.01 mg/kg, i.m.) was administered, and topical antibiotic was applied on a daily basis. Subsequently the animals were adapted to a recording environment for a period of at least two weeks.

2.3. Experimental sessions

Experimental sessions, which were three to four hours in duration, were conducted between 11 A.M. and 3 P.M in a temperature-controlled environment (21-23 °C). During the sessions, the animals' head was held in stereotaxic position by a chronic head-holder; the EEG, EOG, PGO and neck electromyogram (EMG, recorded via pin electrodes that were placed acutely in the neck muscles) were monitored and the data were stored using Superscope® software and a Macintosh® computer. The animals did not exhibit any signs of stress or discomfort during these sessions, as evidenced by their quiescent behavior and the fact that they quickly cycled through states of sleep and wakefulness.

The animals were euthanized with an overdose of sodium pentobarbital (60 mg/kg) immediately after they had spent at least one hour either in state of quiet wakefulness (QW, n = 4), alert wakefulness (AW, n = 3), NREM (n = 4) or REM sleep induced by carbachol (REM-carbachol, n = 6).

In order to produce an extended period that comprised predominantly one behavioral state, the following procedures were undertaken. To generate QW, the EEG was monitored continuously, and if slow activity or spindles appeared in the EEG, low noise or mild somesthetic stimulation was applied.

The experimental procedures for the AW animals were similar to that used for the QW animals; however, they were maintained in an alert state by the delivery of loud clicks of variable intensity (up to 90 dB SPL). This stimulation has been shown to generate alert wakefulness and produce an increase in power of the gamma band of the EEG (Torterolo et al., 2003).

Animals in the NREM group were maintained awake for two to three hours; thereafter, during a period of 60-90 minute prior to euthanasia, there was a robust NREM rebound (Figure 1A). During this time REM sleep was prevented from occurring by low noise or mild somesthetic stimulation when a sequence of PGO waves appeared, indicating that REM sleep was about to occur.

In order to obtain a long duration period of REM sleep, carbachol (0.8 μg in 0.2 μl of saline) was microinjected during NREM into the nucleus pontis oralis (NPO, AP -2 to -3, L 1.5 to 2.5, H -3.5 to -5 (Berman, 1968)), according to procedures that we have previously employed (Torterolo et al., 2000; Torterolo et al., 2009b).

Data were also obtained from two additional animals that were allowed to sleep undisturbed before euthanasia, as well as from one animal that, in the hour prior to euthanasia, exhibited a robust REM sleep rebound (REM-R) that followed a period of REM sleep deprivation (see Figure 1). As is shown in Figure 1, the final experimental session of the REM-R animal was exceptionally long (approximately 6.5 hour, from 8:30 to 3 PM). The data for these three animals was only used for correlation analysis (see Results section).

2.4. Immunohistochemistry

Each animal was perfused with one liter of heparinized saline followed by one and a half liters of a solution of 4% paraformaldehyde, 15% saturated picric acid and 0.5% of glutaraldehyde in phosphate buffer (PB, 0.1 M, pH 7.4). Subsequently, it was perfused with 1.2 liters of the same solution with 10% sucrose. The brain was then removed and immersed in a postfixative solution of 2% paraformaldehyde, 15% saturated picric acid and 10% sucrose in PB for 24 hours. Following postfixation, the tissue was kept for three days in a solution of sucrose (25%) and sodium azide (0.1%) in PB. Afterward, the brain was frozen and brainstem serial sections of 14 μm were obtained using a Reichert-Jung cryostat. These sections were stored in a solution of 0.1% sodium azide in PB-saline (PBS, 0.1 M).

Free-floating sections were incubated overnight in a rabbit polyclonal Fos antiserum (Fos Ab5; Oncogene Research Products) at a dilution of 1:40000 in PBS. The sections were rinsed four times in PBS for 30 minutes and then incubated for 90 minutes in a biotinylated donkey anti-rabbit immunoglobulin G (1:700, Jackson Laboratories). Then, the sections were then incubated with the ABC kit (Vector, 1:500) for 60 minutes. After another rinsing, the tissue was reacted for 10-20 minutes with 0.6% nickel ammonium sulfate, 0.02% diaminobenzidine tetrahydrochloride (DAB, Sigma) and 0.015% hydrogen peroxide in 50 mM tris buffer, pH 7.5.

In order to identify GABAergic neurons, polyclonal guinea pig antibodies raised against GABA–keyhole limpet hemocyanin conjugated with glutaraldehyde (NT-108, Protos) were employed. Sections that were previously treated for Fos were incubated overnight with the GABA antibody (1:3500) and normal donkey serum (NDS; 3%). Thereafter, the sections were rinsed and incubated for 60 min with biotinylated donkey anti-guinea-pig antibody (1:300) plus NDS. After another rinse, the tissue was incubated in the ABC complex (1:200) for 60 min, and then exposed to diaminobenzidine and hydrogen peroxide (without nickel enhancement). Cholinergic and catecholaminergic neurons were identified utilizing choline acetyltransferase, (ChAT, Chemicon, 1:2000) and tyrosine hidroxilase (TH, Chemicon, 1:2000) primary antibodies, respectively. The immunoreactions were visualized by procedures that were similar than the one utilized to reveal GABA. Similar immunohistochemical procedures have been employed in our previous studies (Torterolo et al., 2000, 2001; Torterolo et al., 2002; Torterolo et al., 2009a).

All sections were mounted onto superfrost slides; selected sections were counterstained with Pyronin-y to highlight neuronal cytoplasm.

2.5. Data analysis

The states of sleep and wakefulness were determined on the basis of polygraphic records that were stored using the Superscope program and a Macintosh computer. The recordings were then analyzed according to standard criteria for state determinations (Ursin and Sterman, 1981). The frontal EEG was analyzed using a Fast Fourier Transform (FFT). Power values were obtained for consecutive 10 seconds epochs in the delta (0.5 to 4 Hz), theta (4.5 to 8.5 Hz), sigma (9 to 14 Hz), beta (14.5 to 30 Hz) and gamma (30.5 to 50 Hz) frequency bands. The power in each band, as a percentage of the total power, was calculated for consecutive 10 seconds epochs. Sequential 10 seconds epochs of the rectified EOG and EMG were also determined.

Sections of the brainstem were examined by light microscopy; photomicrographs were obtained using a SPOT digital camera attached to an Olympus BX60 microscope. Images were analyzed on a Power Macintosh G4 computer using Adobe PhotoShop software. The number and distribution of immunolabeled neurons were determined from drawings using a camera lucida attachment. In order to perform cell counts, six representative coronal

hemisections separated by approximately 100 μm were selected for each cat at the level of the CLPB (P 3-3.5, L 4 to 5.2, and H -2.5 to -4.5, according to (Berman, 1968)). A rectangular grid area of 2 mm dorso-ventrally and 1 mm medio-laterally was utilized for counting purposes; the superior-external corner of the grid was located approximately at P 3-3.5, L 5, H -2.5 (Figure 2). Cell counts were averaged to yield one value per cat.

Cell counts are reported as the mean ± S.D. The statistical significance between the mean numbers of Fos + neurons in the different behavioral conditions was evaluated utilizing the one-way analysis of variance (ANOVA) and Bonferroni *post-hoc* tests. The number of GABA+Fos+ neurons during NREM sleep and QW was compared using the unpaired two-tailed Student's t test. The criterion chosen to discard the null hypothesis was $P < 0.05$. Correlation analyses using the Pearson correlation coefficient were carried out for the entire population of animals (n = 20) between the percentages of time spent in each behavioral state one hour prior to euthanasia, and the number of Fos+ neurons. Neuronal size was determined by measuring the major and minor diameters of Fos+ and Fos- cells in the NREM group of animals in Pyronin-y counterstained sections.

3. Results

3.1. Sleep characteristics

The NREM group of animals spent an average of 85% of the hour prior to euthanasia in NREM. These animals also exhibited occasional short episodes of quiet wakefulness that lasted less than one or two minutes. Figure 1A shows the hypnogram, EEG frequency bands power and the rectified EMG of a representative NREM animal. The increment in delta and sigma power in correlation with the decrease in gamma power confirmed that this animal spent most of the last experimental hour in NREM.

The QW and AW groups of animals spent most of the time in the waking state throughout the experimental session. Only short periods of light NREM (< 7% the hour prior to euthanasia) interrupted the waking state.

In the REM-carbachol group of animals, carbachol produced an REM sleep-like state with a latency of 4.8 ± 4.1 minutes and duration of 91.4 ± 24.2 minutes. During this state, the animals exhibited typical behavioral characteristics of REM sleep; their eyes were closed and they lay on their side without gross body movements. In addition, EEG desyncronization, rapid eyes movements, PGO waves and muscle atonia were present. A representative example of an animal in the REM-carbachol state was presented in a previous report from our group (Torterolo et al., 2006).

During the hour prior to euthanasia, the "undisturbed" animals spent, on average, 43% of the time in NREM and 57% in W (no REM sleep), while the REM-R animal spent 59.7% of the time in REM sleep and 36.9% in NREM. The hypnogram, EEG frequency bands powers and the rectified EMG of this animal are presented in Figure 1B. The strong REM sleep rebound in the last hour of the recording is readily observed.

3.2. Fos immunoreactivity

All NREM animals exhibited a dense cluster of Fos+ neurons in the CLPB, whereas very few Fos immunoreactive neurons were observed in other areas of the brainstem. In Figure 2, a large number of Fos+ neurons in the CLPB is shown in sections from two representative NREM animals; Fos which is labeled in black, is concentrated in the cells' nuclei. Fos immunoreactivity in the same area of a QW animal is presented for comparison; very few Fos+ neurons were observed in the CLPB in QW animals. As shown in the camera lucida

drawings of Figure 3, the area of Fos immunoreactivity during NREM, which was relatively small, was centered at P 3-3.5, caudal, lateral and ventral to the brachium conjunctivum.

The number of Fos immunoreactive neurons in the CLPB was significantly different among conditions ($F_{3, 13} = 68.6$, $P < 0.0001$, ANOVA). *Post hoc* Bonferroni comparison revealed that during NREM the number of Fos+ neurons (67.9 ± 10.9) was significantly greater ($P < 0.0001$) compared to QW (8.0 ± 6.7), AW (5.2 ± 4.2) or REM-carbachol (8.0 ± 4.7) (Figure 4).

A regression plot between the percentage of time spent in NREM and the number of Fos+ neurons in the CLPB is shown in Figure 5. The number of Fos immunoreactive cells in the CLPB significantly increased in relation to the time spent in NREM ($R = 0.93$). On the other hand, there was no significant correlation between the number of Fos+ neurons and the percentage of time spent in W ($R = 0.35$, data not shown).

In Figure 6A and B, CLPB Fos immunoreactive neurons during NREM are shown in sections counterstained with Pyronin-y. In two animals we determined that during NREM sleep the CLPB neurons that expressed *c-fos* were small and oval-shaped with a large diameter of 14.9 ± 2.7 μm and a small diameter of 9.2 ± 2.0 μm. Furthermore, in the same animals we also observed that small ChAT+ neurons as well as medium-sized TH+ neurons were present in the CLPB; however, Fos immunoreactive neurons during NREM sleep were neither cholinergic nor catecholaminergic (Figure 6C and D).

Double immunohistochemistry for GABA and Fos was performed in sections from NREM and QW animals. High magnification photomicrographs of GABA+Fos+ neurons, single labeled GABAergic (GABA+ Fos-) and single-labeled Fos+ neurons (GABA- Fos+) from sections of a NREM animal are shown in Figure 7. Camera lucida drawings of the CLPB obtained from sections of QW and NREM animals are presented in Figure 8; the number of GABA+Fos+ and GABA- Fos+ neurons during NREM is greater than during QW. In fact, there was a larger number of GABAergic neurons with Fos immunoreactivity (GABA+ Fos +, 29.6 ± 11.1, n = 3) during NREM compared with QW (2.1 ± 1.9; $P < 0.005$, n = 3, unpaired two-tailed Student's t test). The number of GABA+Fos+ neurons counted in the CLPB during NREM (29.6 ± 11.1) was about 50% of the total Fos+ neurons (67.9 ± 10.9).

4. Discussion

In the present study, Fos immunoreactivity in the cat brainstem was analyzed during sleep and wakefulness. Although very few Fos immunoreactive neurons were identified throughout the brainstem during NREM, we discovered a group of neurons that expressed *c-fos*, selectively, during NREM; these neurons were located in the CLPB. Although nuclei at this level of the brainstem have been implicated in the control of wakefulness as well as REM sleep (see below), this is the first demonstration that a discrete population of neurons is active during NREM in the mesopontine region.

4.1. Technical considerations

In previous reports, we have employed the expression of the proto-oncogen, *c-fos*, as a marker of neuronal activation in the cat (Yamuy et al., 1993; Torterolo et al., 2000; Torterolo et al., 2009a). The cat is the classical animal that has been used for decades in sleep research; this species can spend 1 to 2 h, which is a period of time compatible with the temporal dynamic of the Fos protein (Dragunow and Faull, 1989; Morgan and Curran, 1991; Yamuy et al., 1993; Hughes and Dragunow, 1995; Cirelli and Tononi, 2000; Kovacs, 2008), in states such as wakefulness, NREM sleep, and in REM sleep when pharmacologically induced.

The synthesis of the Fos protein depends upon the cell type as well as the nature of the stimulus. For example, in vitro studies have shown that following appropriate stimulation, Fos protein levels in quiescent fibroblasts reach a maximum in 30 min and decrease to very low levels at 2 h (Kovary and Bravo, 1991); however it was also demonstrated that the induction of the Fos protein requires a period of up to 90 min to reach its maximum level (reviewed by Cirelli and Tononi, 2000). Nevertheless, Shiromani et al., (1996) successfully employed Fos immunoreactivity in REM-carbachol cats with REM sleep durations ranging from 27 to 40 minutes.

Since 1993 our group has been studying Fos expression in different areas of the cat CNS during states of sleep and wakefulness (Yamuy et al., 1993). Consistently, we have found that the maintenance of these animals for a period of 1 to 2 hours in a specific behavioral state is optimal for Fos expression; we have never observed differences between one or two hours (Yamuy et al., 1998; Torterolo et al., 2003; Torterolo et al., 2006; Torterolo et al., 2009a).

The REM-carbachol state fulfills the polysomnography characteristics of natural REM sleep; i.e., EEG desynchronization, PGO waves, rapid eye movements, muscle atonia due to the presence of glycinergic postsynaptic IPSPs in motoneurons, and the absence of the 40 Hz rhythm of the olfactory bulb that occurs during wakefulness (Hernandez-Peon et al., 1960; Baghdoyan et al., 1987; Morales et al., 1987; Lopez-Rodriguez et al., 1994). As in physiological REM sleep, respiratory depression and hippocampal theta rhythm are also present during REM-carbachol (Lydic and Baghdoyan, 1989; Lopez-Rodriguez et al., 1994).

4.2. Neurons that express Fos during NREM sleep in the cat

Fos expression in the pons and medulla of the cat has been studied in detailed by Yamuy et al. (1993). Fos-immunoreactive neurons were observed throughout these regions both during wakefulness and REM-carbachol. We have also shown that GABAergic neurons of mesopontine regions medial to the CLPB, such as the laterodorsal and pedunculo pontine tegmental nuclei (LDT-PPT), dorsal raphe nucleus and dorsal tegmental nucleus of Gudden, express Fos either in wakefulness and/or REM-carbachol (Torterolo et al., 2000, 2001; Torterolo et al., 2002). In the present report, we found in the brainstem of the cat during NREM sleep that only in the CLPB there is a dense cluster of Fos-immunoreactive neurons. Immunoreactivity for Fos was not observed in the area of the solitary tract that is involved in functions during NREM sleep (Magnes et al., 1961).

In a previous report, we also analyzed Fos immunoreactivity in the preoptic area of the cat, a critical area for NREM sleep generation (Torterolo et al., 2009a). Interestingly, although there were neurons active in the ventro-lateral preoptic nucleus (VLPO) during NREM sleep, the number of Fos + neurons was not greater during NREM sleep compared with other behavioral states (Torterolo et al., 2009a). On the contrary, in the median preoptic nucleus (mPOA), the number of Fos immunoreactive neurons increased during NREM sleep. It would be important to know if there are any functional relationships between the mPOA and CLPB NREM sleep-related neurons.

In the lateral hypothalamus, melanin concentrating hormone (MCH)-containing neurons that are involved in sleep regulation (Torterolo et al., 2011), did not express Fos during NREM in the cat (Torterolo et al., 2006).

4.3. The caudolateral peribrachial region: anatomy and function

The parabrachial region surrounding the brachium conjunctivum is divided into 13 distinct subnuclei in the rat, each associated with a unique set of afferents, efferents and neurotransmitters (Saper, 1995). The area where we observed Fos immunoreactivity during

NREM is identified as the CLPB (Datta, 1997; Quattrochi et al.). This area includes part of the marginal nucleus of the brachium conjunctivum as well as the dorsal region of the Kolliker Fuse nucleus (Berman, 1968).

The CLPB is innervated by afferents from the preoptic region and the nucleus of the solitary tract (Takeuchi and Hopkins, 1984; Simerly and Swanson, 1988; Herbert et al., 1990; Herbert and Saper, 1990; Moga et al., 1990a; Moga et al., 1990b; Saper, 1995; Zardetto-Smith and Johnson, 1995); both of these areas that have been implicated in the generation and/or maintenance of NREM (Magnes et al., 1961; Szymusiak and McGinty, 2008).

A small number of cholinergic and catecholaminergic neurons have been identified in the CLPB (Jones and Beaudet, 1987; Reiner and Vincent, 1987), but the neurons that were found to be active during NREM were neither cholinergic nor catecholaminergic. On the other hand, a portion (roughly 50%) of the NREM+Fos+ neurons consisted of GABAergic cells. Additional experiments are required to determine the neurotransmitters phenotype(s) of the remaining NREM-selective Fos+ neurons in the CLPB, which are neither GABAergic, cholinergic nor cathecolaminergic.

The CLPB and adjacent parabrachial areas are also components of the central autonomic network; which function as an interface between the medullary and forebrain regulation of the autonomic processes (Saper, 1995). For example, there are direct projections from the CLPB and adjacent parabrachial subnuclei to sympathetic preganglionic columns in the spinal cord, and large increases in blood pressure are produced by electrical or chemical stimulation of the CLPB (Saper, 1995). In addition, this area is involved in the regulation of breathing (Chamberlin, 2004).

4.4. The mesopontine region is involved in the generation of wakefulness and REM sleep

As mentioned in the Introduction, there are several reports that have demonstrated that mesopontine regions generate either wakefulness or REM sleep, but not NREM.

The NPO of the cat or its corresponding nucleus in the rat, which is called the sub-laterodorsal nucleus, is an integral part of different models of REM sleep, and is considered to exert executive control over the initiation and maintenance of REM sleep (Reinoso-Suarez et al., 2001; Chase and Morales, 2005; Siegel, 2005; Fuller et al., 2007; Luppi et al., 2007; McCarley, 2007). A single injection of a cholinergic agonist, such as carbachol, induces an extraordinary behavioral response in the cat, which is the generation of REM sleep with a very short latency (occasionally within 30 s) together with durations that can exceed 2 h (George et al., 1964; Baghdoyan et al., 1987; Garzon et al., 1998). An example of an REM-carbachol episode of 2 hours duration was presented in Torterolo et al., (2006). Cholinergic REM sleep-on neurons of the LDT-PPT also play a critical role in the promotion of REM sleep; the release of acetylcholine from these neurons are believed to activate the cholinoceptive neurons of the NPO through muscarinic receptors (Baghdoyan and Lydic, 1999; Coleman et al., 2004). On the other hand, REM sleep-off neurons monoaminergic neurons of the dorsal raphe nucleus and locus coeruleus have REM sleep suppressive functions (Jones, 2005; McCarley, 2007). Other mesopontine regions such as the ventral periaqueductal gray have been also involved in REM sleep generation (Vanini et al., 2007).

Neurons in the LDT-PPT, part of the ascending reticular activating system, are also involved in the control of wakefulness (Semba, 1999). This nucleus contain cholinergic and non-cholinergic cells that are active during wakefulness and/or REM sleep and project rostrally to thalamic and hypothalamic regions where they modulate neurons that are responsible for activating the EEG (Hallanger et al., 1987; Steriade et al., 1990)

On the contrary, there are very few reports that relate the CLPB with the control of behavioral states (see below).

4.5. Is the caudolateral peribrachial region involved in the control of sleep?

The CLPB has previously been proposed to be responsible for the generation of PGO-waves (Calvo et al., 1992; Datta et al., 1992), a signature pattern of activity that occurs during the NREM-REM sleep transition and during REM sleep. Microinjections of carbachol into the CLPB produce the immediate onset of state-independent PGO waves in the ipsilateral lateral geniculate nucleus (Calvo et al., 1992; Datta et al., 1992). Unilateral neurotoxic lesions or cooling of this area results in a large decrease in ipsilateral PGO-waves (Laurent and Ayala-Guerrero, 1975; Datta and Hobson, 1995). In fact, there are neurons within this region that increase their firing rate preceding the first PGO wave in NREM, and maintain a high frequency rate in correlation with the PGO waves during REM sleep (Datta, 1995). However, in our experiments, CLPB neurons did not express *c-fos* during REM-carbachol a pharmacologically induced state characterized by the presence of PGO-waves. Because the induction of REM sleep by the microinjection of carbachol in the NPO is likely to be "downstream" in the cascade of neuronal events that trigger PGO waves, CLPB neurons may be "bypassed," i.e., not activated during this pharmacologically-induced state.

Ventilation is strongly affected during the transition from NREM to REM sleep (Douglas, 2005; Orem and Kubin, 2005). In addition, during NREM the activity of the autonomic system shifts toward an increase in tonic parasympathetic activity with a decrease in sympathetic drives; this balance changes upon entry into the state of REM sleep, when there is great variability in the activity of both divisions of the autonomic nervous system (Parmeggiani, 2005). In this regard, Parmeggiani proposed that there is a decrease in the hypothalamic control of the autonomic nervous system during REM sleep, and that this decrease results in an increase in the modulation of autonomic processes by rhombencephalic structures, which would be sufficient for the maintenance of cardiovascular and respiratory control, but not for thermoregulation (Parmeggiani, 2005). Therefore, we suggest that the CLPB may play a vital role in the brainstem control of respiratory and automatic processes during NREM, and especially during the transition to REM sleep. In this regard, it is important to point out that, in our experiments, we were not able to determine if the CLPB regulates NREM sleep as a whole or only respiratory or autonomic phenomena during this state.

4.6. Conclusions and future directions

There are several unique characteristics of CLPB neurons; they are involved in the autonomic and respiratory regulation. They are also activated during NREM and their activity has been associated with one of the principal heraldic signs of REM sleep, which is the occurrence of PGO waves. As a working hypothesis, we propose that CLPB neurons play a primary role in coordinating the activities of various central and peripheral systems during NREM and in the transition from NREM to REM sleep. Consequently, we believe that the present data opens new avenues for the study of the control not only of NREM, but also of interactions between brainstem and forebrain sites that are involved in the transition from NREM to REM sleep.

Acknowledgments

This study was supported by USPHS NS09999 grant.

References

Baghdoyan HA, Lydic R. M2 muscarinic receptor subtype in the feline medial pontine reticular formation modulates the amount of rapid eye movement sleep. Sleep. 1999; 22:835–847. [PubMed: 10566902]

Baghdoyan HA, Rodrigo-Angulo ML, McCarley RW, Hobson JA. A neuroanatomical gradient in the pontine tegmentum for the cholinoceptive induction of desynchronized sleep signs. Brain Res. 1987; 414:245–261. [PubMed: 3620930]

Berman, AL. A citoarchitectonic atlas with stereotaxic coordinates. University of Wisconsin; Madison: 1968. The brain stem of the cat.

Calvo JM, Datta S, Quattrochi J, Hobson JA. Cholinergic microstimulation of the peribrachial nucleus in the cat. II. Delayed and prolonged increases in REM sleep. Arch Ital Biol. 1992; 130:285–301. [PubMed: 1489249]

Chamberlin NL. Functional organization of the parabrachial complex and intertrigeminal region in the control of breathing. Respir Physiol Neurobiol. 2004; 143:115–125. [PubMed: 15519549]

Chase, M.; Morales, FR. Control of motoneurons during sleep. In: Kryger, MH., et al., editors. Principles and practices of sleep medicine. Elsevier-Saunders; Philadelphia: 2005. p. 154-168.

Cirelli C, Tononi G. On the functional significance of c-fos induction during the sleep-waking cycle. Sleep. 2000; 23:453–469. [PubMed: 10875553]

Coleman CG, Lydic R, Baghdoyan HA. M2 muscarinic receptors in pontine reticular formation of C57BL/6J mouse contribute to rapid eye movement sleep generation. Neuroscience. 2004; 126:821–830. [PubMed: 15207317]

Datta S. Neuronal activity in the peribrachial area: relationship to behavioral state control. Neurosci Biobehav Rev. 1995; 19:67–84. [PubMed: 7770199]

Datta S. Cellular basis of pontine ponto-geniculo-occipital wave generation and modulation. Cell Mol Neurobiol. 1997; 17:341–365. [PubMed: 9187490]

Datta S, Calvo JM, Quattrochi J, Hobson JA. Cholinergic microstimulation of the peribrachial nucleus in the cat. I. Immediate and prolonged increases in ponto-geniculo-occipital waves. Arch Ital Biol. 1992; 130:263–284. [PubMed: 1489248]

Datta S, Hobson JA. Suppression of ponto-geniculo-occipital waves by neurotoxic lesions of pontine caudo-lateral peribrachial cells. Neuroscience. 1995; 67:703–712. [PubMed: 7675196]

Dentico D, Amici R, Baracchi F, Cerri M, Del Sindaco E, Luppi M, Martelli D, Perez E, Zamboni G. c-Fos expression in preoptic nuclei as a marker of sleep rebound in the rat. Eur J Neurosci. 2009; 30:651–661. [PubMed: 19686475]

Douglas, N. Respiratory Physiology: control of ventilation. In: Kryger, MH., et al., editors. Principles and practices of sleep medicine. Elsevier-Saunders; Philadelphia: 2005. p. 224-231.

Dragunow M, Faull R. The use of c-fos as a metabolic marker in neuronal pathway tracing. J Neurosci Methods. 1989; 29:261–265. [PubMed: 2507830]

Fuller PM, Saper CB, Lu J. The pontine REM switch: past and present. J Physiol. 2007; 584:735–741. [PubMed: 17884926]

Garzon M, De Andres I, Reinoso-Suarez F. Sleep patterns after carbachol delivery in the ventral oral pontine tegmentum of the cat. Neuroscience. 1998; 83:1137–1144. [PubMed: 9502252]

George R, Haslett W, Jenden D. A cholinergic mechanism in the brainstem reticular formation: induction of paradoxical sleep. Int J Neuropharmacol. 1964; 3:541–552. [PubMed: 14344492]

Gong H, Szymusiak R, King J, Steininger T, McGinty D. Sleep-related c-Fos protein expression in the preoptic hypothalamus: effects of ambient warming. Am J Physiol Regul Integr Comp Physiol. 2000; 279:R2079–2088. [PubMed: 11080072]

Hallanger AE, Levey AI, Lee HJ, Rye DB, Wainer BH. The origins of cholinergic and other subcortical afferents to the thalamus in the rat. J Comp Neurol. 1987; 262:105–124. [PubMed: 2442206]

Herbert H, Moga MM, Saper CB. Connections of the parabrachial nucleus with the nucleus of the solitary tract and the medullary reticular formation in the rat. J Comp Neurol. 1990; 293:540–580. [PubMed: 1691748]

Herbert H, Saper CB. Cholecystokinin-, galanin-, and corticotropin-releasing factor-like immunoreactive projections from the nucleus of the solitary tract to the parabrachial nucleus in the rat. J Comp Neurol. 1990; 293:581–598. [PubMed: 1691749]

Hernandez-Peon R, Lavin A, Alcocer-Cuaron C, Marcelin JP. Electrical activity of the olfactory bulb during wakefulness and sleep. Electroencephalogr Clin Neurophysiol. 1960; 12:41–58. [PubMed: 14401279]

Hughes P, Dragunow M. Induction of immediate-early genes and the control of neurotransmitter-regulated gene expression within the nervous system. Pharmacological reviews. 1995; 42:133–178. [PubMed: 7784478]

Jones, B. Basic mechanisms of sleep-wake states. In: Kryger, MH., et al., editors. Principles and practices of sleep medicine. Elsevier-Saunders; Philadelphia: 2005. p. 136-153.

Jones BE, Beaudet A. Distribution of acetylcholine and catecholamine neurons in the cat brainstem: a choline acetyltransferase and tyrosine hydroxylase immunohistochemical study. J Comp Neurol. 1987; 261:15–32. [PubMed: 2887593]

Kovacs KJ. Measurement of immediate-early gene activation- c-fos and beyond. J Neuroendocrinol. 2008; 20:665–672. [PubMed: 18601687]

Kovary K, Bravo R. Expression of different Jun and Fos proteins during the G0-to-G1 transition in mouse fibroblasts: in vitro and in vivo associations. Mol Cell Biol. 1991; 11:2451–2459. [PubMed: 1901942]

Laurent JP, Ayala-Guerrero F. Reversible suppression of ponto-geniculo-occipital waves by localized cooling during paradoxical sleep in cats. Exp Neurol. 1975; 49:356–369. [PubMed: 172364]

Lopez-Rodriguez F, Kohlmeier K, Morales FR, Chase MH. State dependency of the effects of microinjection of cholinergic drugs into the nucleus pontis oralis. Brain Res. 1994; 649:271–281. [PubMed: 7953643]

Luppi PH, Gervasoni D, Verret L, Goutagny R, Peyron C, Salvert D, Leger L, Fort P. Paradoxical (REM) sleep genesis: The switch from an aminergic-cholinergic to a GABAergic-glutamatergic hypothesis. Journal of Physiology (Paris). 2007; 100:271–283.

Lydic R, Baghdoyan HA. Cholinoceptive pontine reticular mechanisms cause state-dependent respiratory changes in the cat. Neurosci Lett. 1989; 102:211–216. [PubMed: 2812500]

Magnes J, Moruzzi G, Pompeiano O. Synchronization of EEG produced by low-frequency electrical stimulation of the region of the solitary tract. Arch Ital Biol. 1961; 99:33–67.

McCarley RW. Neurobiology of REM and NREM sleep. Sleep Med. 2007; 8:302–330. [PubMed: 17468046]

Moga MM, Herbert H, Hurley KM, Yasui Y, Gray TS, Saper CB. Organization of cortical, basal forebrain, and hypothalamic afferents to the parabrachial nucleus in the rat. J Comp Neurol. 1990a; 295:624–661. [PubMed: 1694187]

Moga MM, Saper CB, Gray TS. Neuropeptide organization of the hypothalamic projection to the parabrachial nucleus in the rat. J Comp Neurol. 1990b; 295:662–682. [PubMed: 1972710]

Morales FR, Engelhardt JK, Soja PJ, Pereda AE, Chase MH. Motoneuron properties during motor inhibition produced by microinjection of carbachol into the pontine reticular formation of the decerebrate cat. J Neurophysiol. 1987; 57:1118–1129. [PubMed: 3585456]

Morgan JI, Curran T. Stimulus-transcription coupling in the nervous system: involvement of the inducible proto-oncogenes fos and jun. Annu Rev Neurosci. 1991; 14:421–451. [PubMed: 1903243]

Orem, J.; Kubin, L. Respiratory physiology:central neural control. In: Kryger, MH., et al., editors. Principles and practices of sleep medicine. Vol. 213-223. Elsevier-Saunders; Philadelphia: 2005.

Parmeggiani, PL. Physiologic regulation in sleep. In: Kryger, MH., et al., editors. Principles and practices of sleep medicine. Elsevier-Saunders; Philadelphia: 2005. p. 185-191.

Quattrochi J, Datta S, Hobson JA. Cholinergic and non-cholinergic afferents of the caudolateral parabrachial nucleus: a role in the long-term enhancement of rapid eye movement sleep. Neuroscience. 1998; 83:1123–1136. [PubMed: 9502251]

Reiner PB, Vincent SR. Topographic relations of cholinergic and noradrenergic neurons in the feline pontomesencephalic tegmentum: an immunohistochemical study. Brain Res Bull. 1987; 19:705–714. [PubMed: 2894238]

Reinoso-Suarez F, de Andres I, Rodrigo-Angulo ML, Garzon M. Brain structures and mechanisms involved in the generation of REM sleep. Sleep Med Rev. 2001; 5:63–77. [PubMed: 12531045]

Saper, CB. Central autonomic system. In: Paxinos, G., et al., editors. The rat nervous system. Academic Press; London: 1995. p. 107-135.

Semba, K. The mesopontine cholinergic system: a dual role in REM sleep and wakefulness. In: Lydic, R.; Baghdoyan, H., editors. Handbook of behavioral state control. CRC Press; Washington: 1999.

Sherin JE, Shiromani PJ, McCarley RW, Saper CB. Activation of ventrolateral preoptic neurons during sleep. Science. 1996; 271:216–219. [PubMed: 8539624]

Shiromani PJ, Winston S, McCarley RW. Pontine cholinergic neurons show Fos-like immunoreactivity associated with cholinergically induced REM sleep. Brain Res Mol Brain Res. 1996; 38:77–84. [PubMed: 8737670]

Siegel, JM. REM Sleep. In: Kryger, MH., et al., editors. Principles and practices of sleep medicine. Elsevier-Saunders; Philadelphia: 2005. p. 120-135.

Simerly RB, Swanson LW. Projections of the medial preoptic nucleus: a Phaseolus vulgaris leucoagglutinin anterograde tract-tracing study in the rat. J Comp Neurol. 1988; 270:209–242. [PubMed: 3259955]

Steriade M, Datta S, Pare D, Oakson G, Curro Dossi RC. Neuronal activities in brainstem cholinergic nuclei related to tonic activation processes in thalamocortical systems. J Neurosci. 1990; 10:2541–2559. [PubMed: 2388079]

Szymusiak R, Alam N, Steininger TL, McGinty D. Sleep-waking discharge patterns of ventrolateral preoptic/anterior hypothalamic neurons in rats. Brain Res. 1998; 803:178–188. [PubMed: 9729371]

Szymusiak R, McGinty D. Hypothalamic regulation of sleep and arousal. Ann N Y Acad Sci. 2008; 1129:275–286. [PubMed: 18591488]

Takeuchi Y, Hopkins DA. Light and electron microscopic demonstration of hypothalamic projections to the parabrachial nuclei in the cat. Neurosci Lett. 1984; 46:53–58. [PubMed: 6728329]

Torterolo P, Benedetto L, Lagos P, Sampogna S, Chase MH. State-dependent pattern of Fos protein expression in regionally-specific sites within the preoptic area of the cat. Brain Res. 2009a; 1267:44–56. [PubMed: 19269274]

Torterolo P, Lagos P, Monti JM. Melanin-concentrating hormone (MCH): a new sleep factor? Front Neurol. 2011; 2:14. [PubMed: 21516258]

Torterolo P, Sampogna S, Chase MH. MCHergic projections to the nucleus pontis oralis participate in the control of active (REM) sleep. Brain Res. 2009b; 1268:76–87. [PubMed: 19269278]

Torterolo P, Sampogna S, Morales FR, Chase MH. Gudden's dorsal tegmental nucleus is activated in carbachol-induced active (REM) sleep and active wakefulness. Brain Res. 2002; 944:184–189. [PubMed: 12106678]

Torterolo P, Sampogna S, Morales FR, Chase MH. MCH-containing neurons in the hypothalamus of the cat: Searching for a role in the control of sleep and wakefulness. Brain Res. 2006; 1119:101–114. [PubMed: 17027934]

Torterolo P, Vanini G. Nuevos conceptos sobre la generación y el mantenimiento de la vigilia. Revista de Neurología. 2010; 50:747–758.

Torterolo P, Yamuy J, Sampogna S, Morales FR, Chase MH. GABAergic neurons of the cat dorsal raphe nucleus express c-fos during carbachol-induced active sleep. Brain Res. 2000; 884:68–76. [PubMed: 11082488]

Torterolo P, Yamuy J, Sampogna S, Morales FR, Chase MH. GABAergic neurons of the laterodorsal and pedunculopontine tegmental nuclei of the cat express c-fos during carbachol-induced active sleep. Brain Res. 2001; 892:309–319. [PubMed: 11172778]

Torterolo P, Yamuy J, Sampogna S, Morales FR, Chase MH. Hypocretinergic neurons are primarily involved in activation of the somatomotor system. Sleep. 2003; 1:25–28. [PubMed: 12627728]

Ursin, R.; Sterman, M. Manual for standardized scoring of sleep and waking states in adult cats. BIS/BRI, University of California; Los Angeles: 1981.

Vanini G, Torterolo P, McGregor R, Chase MH, Morales FR. GABAergic processes in the mesencephalic tegmentum modulate the occurrence of active (rapid eye movement) sleep in guinea pigs. Neuroscience. 2007; 145:1157–1167. [PubMed: 17346896]

Von Economo C. Sleep as a problem of localization. J Nerv Ment Dis. 1930; 71:249–259.

Yamuy J, Mancillas JR, Morales FR, Chase MH. C-fos expression in the pons and medulla of the cat during carbachol- induced active sleep. J Neurosci. 1993; 13:2703–2718. [PubMed: 8501533]

Yamuy, J.; Sampogna, S.; Morales, FR.; Chase, MH. c-fos expression in mesopontine noradrenergic and cholinergic neurons of the cat during carbachol-induced active sleep: A double labeling study. 1998. Sleep Res Online 1: 28-40, http://www.sro.org/1998/Yamuy/1928/

Zardetto-Smith AM, Johnson AK. Chemical topography of efferent projections from the median preoptic nucleus to pontine monoaminergic cell groups in the rat. Neurosci Lett. 1995; 199:215–219. [PubMed: 8577401]

Abbreviations

AW	alert wakefulness
ChAT	choline acetyltransferase
CLPB	caudolateral peribrachial regio
DAB	diaminobenzidine tetrahydrochloride
EEG	electroencephalogram
EMG	electromyogram
EOG	electro-oculogram
FFT	Fast Fourier Transform
LDT-PPT	laterodorsal and pedunculo pontine tegmental nuclei
NDS	normal donkey serum
NPO	nucleus pontis oralis
NREM	non REM sleep
PB	phosphate buffer
PBS	phosphate buffer-saline
PGO	ponto-geniculo-occipital
QW	quiet wakefulness
REM	rapid eye movements
REM-carbachol	REM sleep induced by carbachol
REM-R	REM sleep rebound
TH	tyrosine hidroxilase

Research Highlights

- Fos immunoreactivity was studied in the brain stem of the cat during sleep.
- Fos+ neurons were observed in the peribrachial region (CLPB) during quiet sleep.
- Fos+ neurons in the CLPB were neither cholinergic nor catecholaminergic.
- Approximately 50% of these neurons were GABAergic.

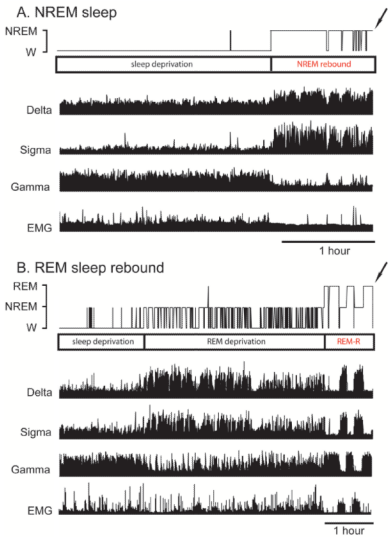

Figure 1.

Characteristics of NREM sleep and REM sleep rebound (REM-R) cats. A. A hypnogram, delta, sigma and gamma power bands, as well as the rectified EMG of a representative NREM cat are shown. Note that after two hours of total sleep deprivation, a period of NREM rebound occurred. REM sleep was not present during this period of time. B. The hypnogram, power in the EEG bands and the rectified EMG of the REM-R animal are also presented. Note the striking fragmentation of NREM, which increased during the period of REM sleep deprivation. Brief awakenings were induced to prevent the animal from entering into REM sleep. During the hour preceding euthanasia, there was an REM sleep rebound. The arrows indicate the time of euthanasia. In order to highlight the relative amplitude of the EEG bands and EMG in relation to behavioral states, the calibration and units were not included in the figure.

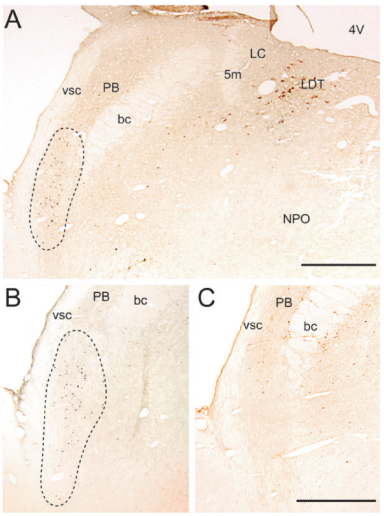

Figure 2.

Fos immunoreactivity in the caudolateral peribrachial (CLPB) region. The photomicrographs exhibit Fos immunoreactivity in two NREM sleep cats (A and B), and in one quiet wakefulness (QW) cat (C). The sections were double immunostained for choline acetyltransferase (ChAT) and Fos. Fos immunoreactivity was observed in the caudolateral zone of the peribrachial region (encircled by dash-lines) during NREM (A and B) but not during QW (C). In A, the photomicrograph includes the caudal portion of the LDT where cholinergic neurons are stained in brown. bc, brachium conjunctivum; LC, locus coeruleus; LDT, laterodorsal tegmental nucleus; NPO, nucleus pontis oralis; PB, parabrachial nucleus; vsc, ventral spinocerebellar tract; 4V, forth ventricle; 5m, tract of the mesencephalic trigeminal nucleus. Photomicrographs were obtained from 14 μm sections, which were processed for immunohystochemistry utilizing the ABC-DAB method. Fos immunostaining was enhanced by nickel. Calibration bars, 1 mm.

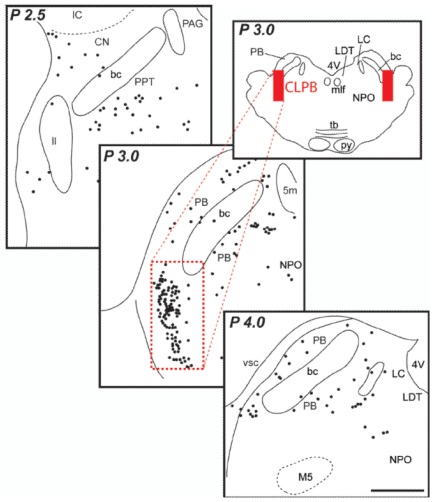

Figure 3.

Rostro-caudal distribution of Fos immunoreactive cells in the CLPB. Camera lucida drawing of Fos immunoreactive neurons in the CLPB during NREM in one representative animal. The counting grid of the CLPB (in red) was located approximately at P 3, L 4 to 5.2, and H -2.5 to -4.5 according to Berman's atlas (Berman, 1968). Very few Fos immunoreactive neurons were located dorsal, ventral or medial to this region. Each dot represents one Fos+ neuron. bc, brachium conjunctivum; CLPB, caudolateral parabrachial area; CN, cuneiform nucleus; IC, inferior colliculus; LC, locus coeruleus; LDT, laterodorsal tegmental nucleus; ll, lateral lemniscus; mlf, medial longitudinal fascicle; M5, motor nucleus of the 5th nerve; NPO, nucleus pontis oralis; PB, parabrachial nucleus; PPT, pedunculo-pontine tegmental nucleus; Py, pyramidal tract; tb, trapezoid body; vsc, ventral spinocerebellar tract; 4V, forth ventricle; 5m, tract of the mesencephalic trigeminal nucleus. Calibration bar, 1 mm.

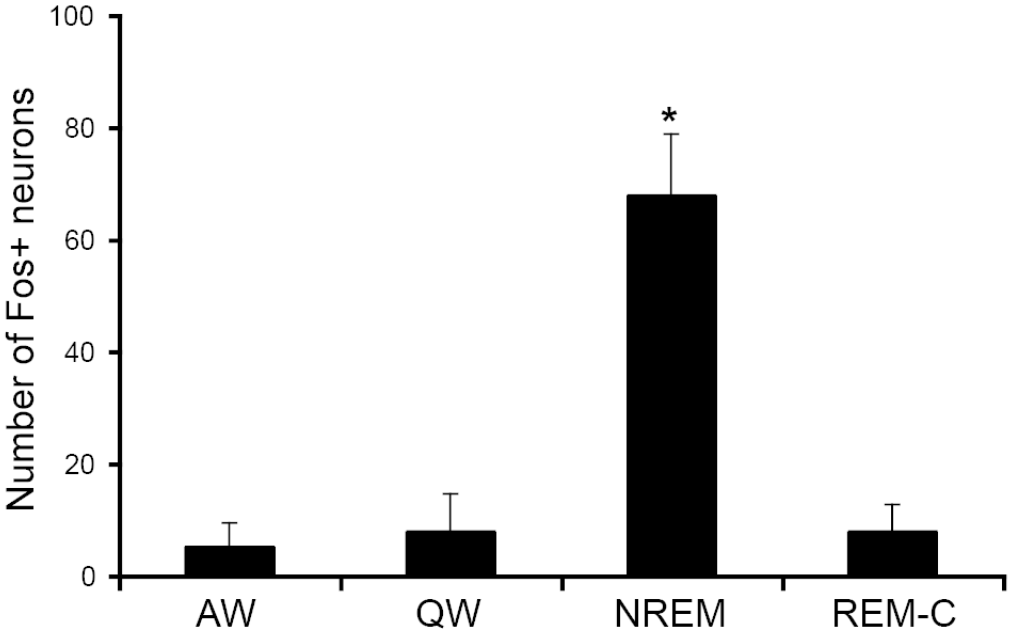

Figure 4.

Bar chart of the mean number of Fos immunoreactive neurons in the caudolateral peribrachial region during different behavioral states. During NREM sleep (n = 4), the number of Fos+ neurons was greater compared to quiet wakefulness (QW, n = 4), alert wakefulness (AW, n =3) and REM-carbachol (REM-C, n = 6). The data was analyzed by ANOVA ($F_{3, 13} = 68.6$) and Bonferroni *post hoc* tests; *, $P < 0.0001$ compared to QW, AW and REM-carbachol.

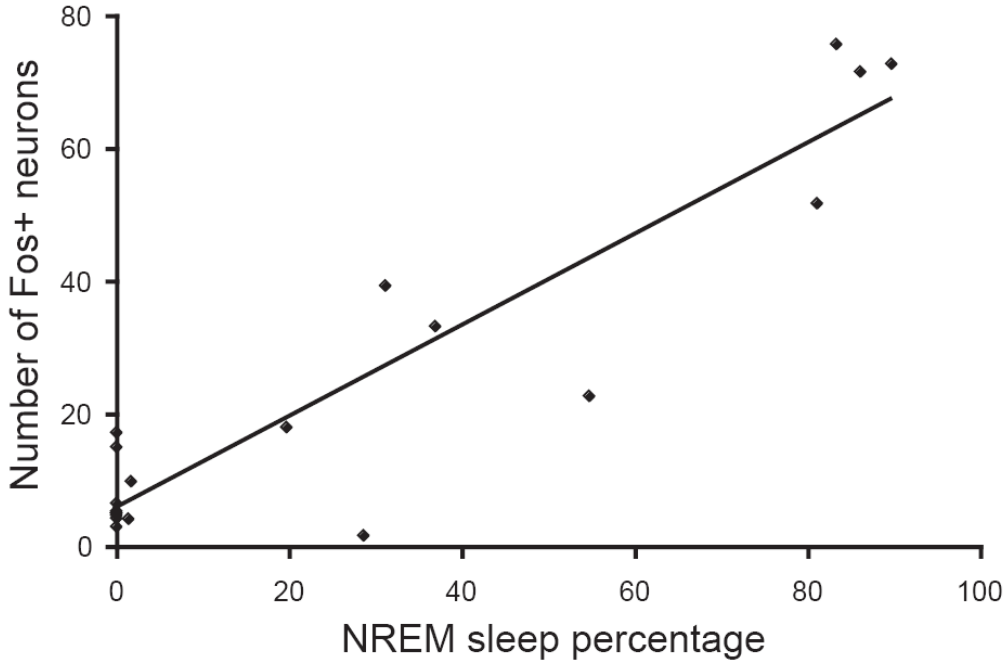

Figure 5.

Regression plot that shows the relation between the percentages of NREM sleep one hour prior to euthanasia and the number of Fos+ neurons in the CLPB. Each dot represents to one animal (n = 20). The regression line corresponds to Y = 0.87X + 5.18. There was a significant correlation between both variables, $P < 0.0001$, R = 0.93.

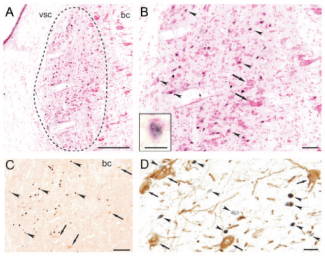

Figure 6.

Characterization Fos+ neurons in CLPB during quiet sleep. Photomicrographs in sections counterstained with Pyronin-Y illustrate Fos immunoreactivity in the CLPB of a NREM cat. In A and B, the same section is shown at different levels of magnification. Fos immunoreactive cells were small (arrowheads), while relatively large neurons (arrows) were Fos-negative. In the inset, a Fos immunoreactive neuron is shown at high magnification. C. Photomicrograph of a section, immunostained for Fos and choline acetyltransferase (ChAT) from a NREM animal. Small cholinergic neurons were present in this and neighboring areas (arrows); Fos immunoreactive neurons were non-cholinergic (arrowheads). D. Photomicrograph of a section from a NREM animal that was immunostained for Fos and tyrosine hydroxylase (TH). Relatively large TH+ neurons were present in the CLPB (arrows); however, Fos immunoreactive neurons were not TH+ (catecholaminergic, arrowheads). bc, brachium conjunctivum; vsc, ventral spinocerebellar tract. Calibration bars: A, 250 μm; B, 50 μm, inset, 25 μm; C, 100 μm; D, 30 μm.

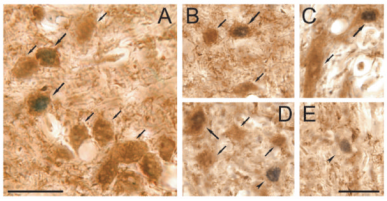

Figure 7.

GABAergic neurons in the CLPB that express *c-fos* during NREM sleep. A to E. Photomicrographs of sections immunostained for Fos and GABA from a NREM animal. A, B and C. GABA+Fos+ (long arrows) and GABA+Fos- (short arrows) neurons were intermingled in this region. D and E. Non-GABAergic Fos+ neurons (arrowheads) were also present within the CLPB during NREM. These neurons were intermingled with GABA+Fos + and GABA+Fos- neurons. Calibration bars: A, 25 μm; B to E, 25 μm.

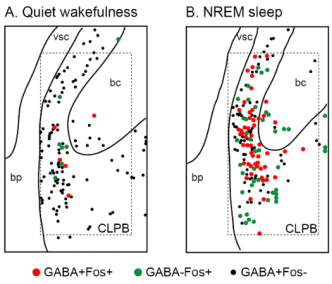

Figure 8.

Camera lucida drawing that shows GABA+Fos+, GABA-Fos+ and GABA+Fos- neurons in two representative animals during NREM sleep and quiet wakefulness (QW). During NREM there is a larger number of GABA+Fos+ and GABA-Fos+ neurons than during QW. bc, brachium conjunctivum; bp, brachium pontis; CLPB, caudolateral parabrachial area; vsc, ventral spinocerebellar tract.